Simplicio, P., Marcos, A., Joffre, E., Zamaro, M., & Silva, N. (2017). Parameterised Laws for Robust Guidance and Control of Planetary Landers. Paper presented at 4th CEAS Specialist Conference on Guidance, Navigation & Control (EURO GNC 2017), Warsaw, Poland.

Peer reviewed version

Parameterised Laws for Robust Guidance and Control of Planetary Landers *

P. Simplício, A. Marcos, E. Joffre, M. Zamaro and N. Silva

Abstract Planetary descent and landing on small planetary bodies are very scientifically rewarding exploration missions but also very challenging from an engineering perspective. This is mostly due to the perturbed and poorly known (physical, gravitational and magnetic) characteristics of the bodies, but also as demonstrated by the European Rosetta mission by the long-time degradation effects of the spacecraft subsystems. In order to address this challenge, the Space community has recognized the need to use robust spacecraft guidance and control algorithms. Of particular relevance, the newly-developed structured $\mathscr{H}_\infty$ design and tuning framework is specially suitable for industry-oriented applications. Specifically for the aforementioned type of Space missions the availability of a fixed GNC architecture coupled with the use of a methodological tuning process and tools is considered a very desirable axis for improvement. In order to apply this GNC tuning advanced tools a structural framework well connected with the industrial state-of-practice and legacy knowledge is required. This paper presents such a parameterised structure for the small planetary bodies' descent and landing exploratory missions, and shows that it reconciles the state-of-the-art in closed-loop guidance techniques.

P. Simplício and A. Marcos
Technology for Aerospace Control, University of Bristol, University Walk, Bristol BS8 1TR, UK
e-mail: pedro.simplicio/andres.marcos @bristol.ac.uk

E. Joffre, M. Zamaro and N. Silva
Airbus Defence and Space Ltd, Gunnels Wood Road, Stevenage SG1 2AS, UK
e-mail: eric.joffre/mattia.zamaro.external/nuno.silva @airbus.com

* This work is jointly funded by the UK Space Agency through a 2016 NSTP-2 Space Technology Fast Track grant entitled "Robust and Nonlinear Guidance and Control for Landing on Small Bodies", as well as by the Engineering and Physical Sciences Research Council (EPSRC)

1 Introduction

Close-proximity operations, including descent and landing, are some of the most critical phases for sample return missions –which are typically characterised by very challenging propellant consumption requirements. While traditional descent strategies involve extended periods of forced motion, significant fuel savings could be achieved by further exploiting the natural dynamics in the vicinity of the target. However, small bodies are characterised by perturbed and poorly known gravitational, physical and magnetic environments, calling for the development of reliable autonomous guidance, navigation and robust control strategies.

The University of Bristol and Airbus Defence and Space have been contracted by the UK Space Agency to specifically investigate advanced robust guidance and control techniques for the design and optimisation of landing trajectories on small planetary bodies. While aiming at a generic framework for the descent and landing on these bodies, the project focuses on Phobos as an illustrative case of the implications of the proposed strategies on system design and operation (for a future interplanetary sample return mission).

As part of the advanced design and optimisation techniques, the project will explore the novel structured $\mathscr{H}_\infty$ optimisation paradigm [2, 12] for the design of robust guidance and control schemes. Structured robust control is a powerful industrially-oriented design and tuning tool, with successful applications rapidly growing. Most notably, it was employed for the refinement of the European Rosetta's orbit controller after thruster authority degradation from its launch ten years before. The retuned control gains were uploaded to the spacecraft just before its braking and final insertion manoeuvres with the target comet in May 2014 [6].

Based on a review of the state-of-art of planetary guidance and control methods, the University of Bristol and Airbus has identified structural commonalities in the guidance laws that seemed not to have been noted before in the best of the author's knowledge. This common structural parameterisation makes them valuable candidates to the application of structured $\mathscr{H}_\infty$ optimisation. The main objective of this paper is thus to highlight the structural commonalities and generalise them into a parameterised (tunable) law which reconciles the planetary guidance state-of-art.

To achieve this objective, the paper is organised as follows: Sec. 2 starts by summarising the state-of-the-art on techniques for planetary descent, Sec. 3 then establishes the mathematical formulation of the planetary descent problem, Sec. 4 presents the parameterised closed-loop laws and demonstrates how they reflect the different strategies identified in the state-of-the-art, and Sec. 5 shows how the proposed parametric generalisation can be applied for guidance tuning. It ends with the main conclusions and future work in Sec. 6.

2 State-of-the-art on Planetary Descent Techniques

In recent years, a renewed interest in small planetary bodies has led to several studies and missions. There are mainly two different purposes behind these studies and missions.

On the one hand, there is the exploitation of hypervelocity impact with a spacecraft as a mitigation strategy against objects in course of potential collision with the Earth. Notable examples of this type of missions include NASA's Deep Impact Spacecraft [21], which successfully hit comet Tempel-1 on July 2005 at 10 km/s, and ESA's Asteroid Impact Mission [7], currently undergoing preliminary design phase but planned to rendezvous with the Didymos binary asteroid system around 2021 (and observe closely the collision with an impactor a few months after).

And on the other hand, there is also the interest of touch-and-go or landing on planetary bodies instead of impacting, as the scientific return in terms of characterisation of these bodies and of the Solar System in general is much higher. Two very successful past missions in this category are JAXA's Hayabusa [29], a sample return mission that landed on Itokawa asteroid on November 2005 returning to Earth five years after, and ESA's Rosetta [13], which performed a rendezvous with comet Churyumov-Gerasimenko and delivered a lander for on-site analysis on November 2014. In addition, NASA has just launched OSIRIS-REx [23], a sample return spacecraft that will reach the near-Earth asteroid Bennu in 2017, and ESA is also studying the feasibility of a sample return mission to Phobos, one of Mars' moons.

In both impact and landing scenarios, an autonomous closed-loop guidance system (in the sense that trajectory is corrected based on onboard measurements) is mandatory to actively characterise the target and perform corrective manoeuvres while coping with very uncertain operational environments. In fact, close-proximity operations around asteroids and comets are very challenging because of their small size, irregular shape and mass distribution, which render their gravitational field very weak, variable and uncertain, with complex orbits stable only in certain regions [22]. Stable trajectories are mostly dependent on the mass ratio between the two main bodies. For example, in the case of Phobos, as this asteroid is very small and very close to Mars, the boundary of its sphere of influence lies just above Phobos' surface and the planet's third-body perturbation cannot be neglected for landing.

The earliest known guidance strategy for the interception of small bodies is actually inspired by the missile interception problem. It is known as proportional navigation guidance (PNG) and introduced in [30], where a method of augmenting it when acceleration characteristics of the target are known or can be assumed is also provided. In addition, guidance using predictive manoeuvres based on linearised orbital perturbation theory [27] is proven possible and complemented with PNG in [14].

However, most of the work on closed-loop guidance for small bodies recasts the problem as optimal feedback control with terminal constraints (no path constraints), which is solved with the Pontryagin minimum principle in [3] or through calculus of variations in [4]. This type of laws, known as optimal guidance laws (OGLs), has been continuously developed for different terminal boundary conditions (con-

strained velocity, free velocity, constrained intercept-angle, etc.) and also related to the classical PNG laws [15, 16, 17, 18].

Additionally, because of the highly uncertain character of the operational environments mentioned above, OGLs have been augmented with nonlinear terms based on sliding mode control (SMC) theory in order to increase their robustness in the presence of inaccurate measurements and unmodelled dynamics [5]. Because of the improved robustness that can be achieved, this research topic has been evolving and applied to different scenarios in the past few years [9, 10].

In parallel, different powered descent strategies have been developed and applied for exploration of larger bodies, such as the Moon and Mars. These approaches are not as demanding as for the asteroid intercept problem since curvature of the planet can often be neglected and its gravity field is relatively uniform and well known. For this reason, the first-generation of Mars probes that successfully reached its surface (from NASA's Viking 1 in 1976 to Phoenix in 2008) relied on an unguided descent phase. As a consequence, these systems generated a landing uncertainty ellipse in the order of 500 km by 100 km [24].

Currently, and in order to be able to fulfil missions with more stringent requirements, several advancements on accurate landing strategies have been taking place, which may bring important contributions to candidate asteroid landing laws. These requirements are typically met through open-loop guidance, in which the complete descent trajectory and thruster profile are generated before the beginning of the manoeuvre. This includes the Apollo program, the next-generation Mars landers (for which the capability of accurately landing spacecraft in hazardous sites with high scientific value, with an uncertainty ellipse down to 100 m [24], is mandatory) and further in the future (or now on Earth) pin-point vertical take-off vertical landing (VTVL) launch vehicles.

Finally, it is noted that the original Apollo guidance law imposed an acceleration profile that is a quadratic function of time [20]. This law was not optimal in the sense that no cost functional was optimised, but the quadratic coefficients were computed analytically from the terminal boundary conditions for a pre-specified descent duration. This approach has been modified in recent times for the NASA's Mars Science Laboratory (MSL) Curiosity in 2011, by adding a line-search over the powered descent duration so as to minimise fuel consumption [28]. However, augmenting the polynomial order of an open-loop guidance law renders the computation of the coefficients under-determined and thus, allows for them to be chosen so as to optimise a desired cost functional. A plethora of optimisation algorithms can be applied to solve this problem and, depending on the method and computational resources available, different path constraints such as minimum altitude or maximum actuation can be explicitly enforced. This is a current very active research topic with notable solutions using either semi-analytical algorithms [25] or convex programming [1].

3 Formulation of the Planetary Descent Problem

The planetary descent configuration with a target asteroid or planet in a standard heliocentric Keplerian orbit is depicted in Fig. 1. It is a simplistic illustration, but the consideration of additional effects is rather straightforward. More specifically, for a descent to Phobos where Mars is the main body, the following applies: 1) non-inertial effects have to be included, 2) gravity forces are non-Keplerian due to the inhomogeneity of the bodies and 3) the gravity of the Sun is only considered as a third-body perturbation.

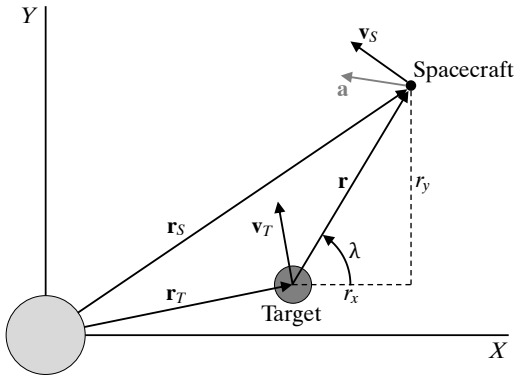

Fig. 1 Problem geometry

The position and velocity of the target in Fig. 1, $\mathbf{r}_T(t) \in \mathbb{R}^3$ and $\mathbf{v}_T(t) \in \mathbb{R}^3$, are then described as follows [17]:

$$\begin{aligned} \dot{\mathbf{r}}_T(t) &= \mathbf{v}_T(t) \\ \dot{\mathbf{v}}_T(t) &= \mathbf{g}_T(\mathbf{r}_T) \end{aligned} \tag{1}$$

where $\mathbf{g}_T(\mathbf{r}_T) \in \mathbb{R}^3$ is the gravitational acceleration acting on the target, which is generically expressed as a partial derivative of the potential gravity of the main body. In addition, $r_T(t) = ||\mathbf{r}_T(t)||$ and $v_T(t) = ||\mathbf{v}_T(t)||$.

Similarly, the position and velocity of the impactor or lander spacecraft in the same frame, $\mathbf{r}_S(t) \in \mathbb{R}^3$ and $r_S(t) = ||\mathbf{r}_S(t)||$, $\mathbf{v}_S(t) \in \mathbb{R}^3$ and $v_S(t) = ||\mathbf{v}_S(t)||$, are modelled as:

$$\begin{aligned} \dot{\mathbf{r}}_S(t) &= \mathbf{v}_S(t) \\ \dot{\mathbf{v}}_S(t) &= \mathbf{g}_S(\mathbf{r}_T, \mathbf{r}_S) + \mathbf{a}(t) + \mathbf{p}(t) \end{aligned} \tag{2}$$

where $\mathbf{g}_S(\mathbf{r}_T, \mathbf{r}_S) \in \mathbb{R}^3$ is the gravitational acceleration felt by the spacecraft, $\mathbf{a}(t) \in \mathbb{R}^3$ is the control acceleration provided by the spacecraft thrusters and $\mathbf{p}(t) \in \mathbb{R}^3$ represents any external perturbations (e.g., solar pressure, gravity inaccuracies) that are typically unknown.

Note that, for this problem, it is assumed that the spacecraft has a dedicated attitude control system, therefore attitude and the aforementioned translational dynamics are considered uncoupled. $\mathbf{g}_S(\mathbf{r}_T, \mathbf{r}_S)$ can be computed with different levels of accuracy, but it will mostly account for the gravity of the main body and of the target on the spacecraft.

Defining the relative position and velocity as $\mathbf{r}(t) = \mathbf{r}_S(t) - \mathbf{r}_T(t)$ and $\mathbf{v}(t) = \mathbf{v}_S(t) - \mathbf{v}_T(t)$, the relative motion between spacecraft and target is expressed as:

$$\begin{aligned} \dot{\mathbf{r}}(t) &= \mathbf{v}(t) \\ \dot{\mathbf{v}}(t) &= \mathbf{g}_S(\mathbf{r}_T, \mathbf{r}_S) - \mathbf{g}_T(\mathbf{r}_T) + \mathbf{a}(t) + \mathbf{p}(t) \end{aligned} \tag{3}$$

with apparent gravitational acceleration $\mathbf{g}(\mathbf{r}_T, \mathbf{r}_S) = \mathbf{g}_S(\mathbf{r}_T, \mathbf{r}_S) - \mathbf{g}_T(\mathbf{r}_T)$ and closing velocity $V_c(t) = -||\mathbf{v}(t)||$.

Following the definitions given above, the descent guidance problem lies on the determination of the acceleration law $\mathbf{a}(t)$ between $t = t_0$ and $t = t_f$ that must:

- Bring the relative states from the terminal boundary conditions $\mathbf{r}(t_0) = \mathbf{r}_0$ and $\mathbf{v}(t_0) = \mathbf{v}_0$ to the final conditions $\mathbf{r}(t_f) = \mathbf{r}_f$ and $\mathbf{v}(t_f) = \mathbf{v}_f$;
- Cope with the effect of external perturbations $\mathbf{p}(t)$ and uncertainties.

The duration from a given instance of time t until the end of the manoeuvre is known as time-to-go, $t_{\text{go}}(t) = t_f - t$. It is also convenient to define the line-of-sight (LOS) vector $\Lambda(t) \in \mathbb{R}^3$ as the direction from target to spacecraft [19]:

$$\Lambda(t) = \frac{\mathbf{r}(t)}{r(t)} \tag{4}$$

For the planar simplification of Fig. 1, the LOS is represented by a single angle:

$$\lambda(t) = \arctan\frac{r_y(t)}{r_x(t)}, \qquad \dot{\lambda}(t) = \frac{r_x(t)\dot{r}_y(t) + r_y(t)\dot{r}_x(t)}{r^2(t)} \tag{5}$$

In addition, in order to reconcile the diverse guidance laws it is important to introduce the concept of zero-effort errors that was defined in [5] :

- Zero-effort-miss (ZEM) is the position error at the end of mission if no corrective manoeuvres are made after time t: $\mathbf{ZEM}(t) = \mathbf{r}_f - \mathbf{r}(t_f) \mid \mathbf{a}(\tau) = 0 \; \forall \; \tau \in [t, t_f]$;
- Zero-effort-velocity (ZEV) is the velocity error at the end of mission if no corrective manoeuvres are made after time t: $\mathbf{ZEV}(t) = \mathbf{v}_f - \mathbf{v}(t_f) \mid \mathbf{a}(\tau) = 0 \, \forall \, \tau \in [t, t_f]$.

Position and velocity can be propagated using (3) in the absence of corrective manoeuvres, hence:

$$\begin{aligned} \mathbf{ZEM}(t) &= \mathbf{r}_f - \left[\mathbf{r}(t) + (t_f - t)\mathbf{v}(t) + \int_t^{t_f} (t_f - \tau)\mathbf{g}(\tau)\, \mathrm{d}\tau\right] \\ \mathbf{ZEV}(t) &= \mathbf{v}_f - \left[\mathbf{v}(t) + \int_t^{t_f} \mathbf{g}(\tau)\, \mathrm{d}\tau\right] \end{aligned} \tag{6}$$

To obtain these analytical expressions for ZEM and ZEV, the gravitational acceleration is assumed to be known as an explicit function of time. However, as the acceleration is more generally given as a function of position (3), the computation of ZEM and ZEV has to be approximated or performed numerically [18]. The definition of ZEM and ZEV can also be extended to the case of a non-zero reference acceleration profile $\mathbf{a}(\tau) = \mathbf{a}_{\text{ref}}(\tau)$.

For the development of guidance laws, spacecraft mass is often assumed constant and the control acceleration is assumed unconstrained. These approximations are then tackled by an inner control loop. For detailed dynamical simulations, the actual spacecraft acceleration results from:

$$\mathbf{a}(t) = \frac{\mathbf{T}(t)}{m(t)} \tag{7}$$

in which the available thrust force $\mathbf{T}(t) \in \mathbb{R}^3$ is limited:

$$0 \leq T_{\min} \leq ||\mathbf{T}(t)|| \leq T_{\max} \tag{8}$$

and the mass variation is given by the classical rocket equation:

$$\dot{m}(t) = -\frac{1}{I_{\text{sp}} g_0} ||\mathbf{T}(t)|| \Rightarrow m(t) = m(t_0) \exp\left(-\frac{1}{I_{\text{sp}} g_0} \int_{t_0}^{t_f} ||\mathbf{a}(\tau)|| \, \mathrm{d}\tau \right) \tag{9}$$

where I_{sp} is the specific impulse of the thrusters, g_0 is the gravitational acceleration at the surface of the Earth and $\Delta m = m(t_0) - m(t_f)$ is the fuel mass consumed for the descent manoeuvre.

4 Parameterised Closed-loop Guidance for Planetary Descent

One of the main objectives of the project under which this work was developed is to exploit the application of the novel non-smooth $\mathscr{H}_\infty$ optimisation paradigm described in [2, 12] for the design of closed-loop guidance and control laws for planetary descent. In particular, this paradigm allows to systematically address optimality trade-offs that are often encountered between performance and robustness against operational uncertainties and disturbances. Uncertain and time-varying effects will be captured through linear fractional transformation (LFT) [31] and linear parameter-varying (LPV) [26] models, respectively.

Moreover, the control design paradigm mentioned above allows to keep the structure of a guidance or control law fixed while tuning its parameters against the desired criteria. For this reason, it is very convenient to be able to parameterise candidate laws as a function of its tunable parameters.

Despite the differences amongst the state-of-the-art guidance laws reviewed in Sec. 2, it was recognised that they share a few structural commonalities. The fun-

damental proposition of this paper is therefore to generalise them as parameterised (tunable) laws.

In this sequence, for the GNC design and tuning of planetary landers, the authors propose the formalisation of closed-loop guidance laws in terms of LOS kinematics:

$$\mathbf{a}(t) = \begin{bmatrix} k_r & k_v \end{bmatrix} V_c(t) \begin{bmatrix} \dfrac{\Lambda(t)}{t_{\mathrm{go}}(t)} \\ \dot{\Lambda}(t) \end{bmatrix} - \phi\, \mathbf{f}\left(\Lambda(t), \dot{\Lambda}(t), t_{\mathrm{go}}(t)\right) \tag{10}$$

or, more sophisticatedly, as a function of zero-effort errors:

$$\mathbf{a}(t) = \begin{bmatrix} k_r & k_v \end{bmatrix} \begin{bmatrix} \dfrac{\mathbf{ZEM}(t)}{t_{\mathrm{go}}^2(t)} \\ \dfrac{\mathbf{ZEV}(t)}{t_{\mathrm{go}}(t)} \end{bmatrix} - \phi\, \mathbf{f}\left(\mathbf{ZEM}(t), \mathbf{ZEV}(t), t_{\mathrm{go}}(t)\right) \tag{11}$$

The reader is referred to Sec. 3 for the definition of variables. The two equations above clearly show a fixed structure with a linear component, parameterised through the gains k_r and k_v (the main parameters to be tuned), together with the possibility of augmenting it with a nonlinear function $\mathbf{f}(.)$ of the feedback variables, weighted by the constant ϕ. The nonlinear function can be introduced for improved robustness properties and designed, for example, based on SMC theory.

In addition, it shall be noted that the laws (10) and (11) become singular when $t \to t_f$ (i.e., $t_{\mathrm{go}}(t) \to 0$), which must be prevented. The most simple way to do it is by switching-off the actuation immediately before the end-of-mission. The exact instant of time is computed as a trade-off between allowable zero-effort errors and maximum acceleration capability.

Finally, it shall be remarked that these generalised laws do not encapsulate open-loop guidance descent. Although important developments have taken place with respect to the latter in terms of explicitly enforcing path constraints, these are mostly targeted at larger bodies (see Sec. 2) and not particularly suitable to cope with the high uncertainty of small asteroid operations. Nevertheless, open-loop guidance laws are also directly parameterised, not as a function of any onboard measurement (such as $\Lambda(t)$, $\mathbf{ZEM}(t)$, $\mathbf{ZEV}(t)$ or $t_{\mathrm{go}}(t)$), but as time polynomials:

$$\mathbf{a}(t) = \mathbf{C}_0 + \mathbf{C}_1 t + \ldots + \mathbf{C}_N t^N, \quad N \geq 2 \tag{12}$$

Depending on the choice of their tunable parameters, the closed-loop guidance laws captured by (10) and (11) may present very different properties. The following three subsections are dedicated to the specification of the main groups identified in Sec. 2 from the generalised equations. These are then summarised in Table 1.

4.1 Proportional laws

Simple proportional laws are inspired by the missile interception problem and known as proportional navigation guidance (PNG). These laws and their most basic variations are introduced in [30] and very well described in [16, 18]. The principle of PNG is to drive the LOS rate to zero by applying a proportional acceleration perpendicularly to the LOS direction:

$$\mathbf{a}(t) = nV_c(t)\dot{\Lambda}(t) \tag{13}$$

where n is the effective navigation ratio, a tunable parameter typically chosen between 3 and 5. Smaller values result in reduced fuel consumption whereas larger values are adopted for improved robustness at the expense of larger acceleration commands. This is the particular case of (10) with $k_r = \phi = 0$ and $k_v = n$.

By considering the contribution of the gravitational environment on the guidance, the augmented PNG (APNG) is an improved variant of this law. Furthermore, representing it as a function of ZEM/ZEV allows to concentrate the knowledge of gravitational forces in these terms, leading to:

$$\mathbf{a}(t) = \frac{n}{t_{\mathrm{go}}^2(t)}\mathbf{ZEM}(t) \tag{14}$$

which is no more than (11) with $k_r = n$ and $k_v = \phi = 0$.

4.2 Optimal laws

The evolution of proportional laws into optimal guidance laws (OGLs) began with the recast of the descent problem as optimal feedback control in [3, 4], being later generalised in [15, 17]. Their objective is to find the acceleration profile $\mathbf{a}(t)$ that minimises the actuation effort, formulated as the cost function:

$$J(\mathbf{a}(t)) = \int_t^{t_f} \frac{1}{2}\mathbf{a}^{\mathrm{T}}(\tau)\mathbf{a}(\tau)\,\mathrm{d}\tau \tag{15}$$

subject to the dynamics of the system (3) and terminal boundary conditions introduced in Sec. 3.

If the terminal value of velocity should be constrained (as is the case for a soft landing), the solution of the problem is given by the constrained terminal velocity guidance (CTVG) law:

$$\mathbf{a}(t) = \frac{6}{t_{\mathrm{go}}^2(t)}\mathbf{ZEM}(t) - \frac{2}{t_{\mathrm{go}}(t)}\mathbf{ZEV}(t) \tag{16}$$

which corresponds to (11) with $k_r = 6$, $k_v = -2$ and $\phi = 0$.

When the terminal velocity is not constrained, it simplifies into free terminal velocity guidance (FTVG):

$$\mathbf{a}(t) = \frac{3}{t_{\mathrm{go}}^2(t)}\mathbf{ZEM}(t) \tag{17}$$

and the coefficients of (11) become $k_r = 3$ and $k_v = \phi = 0$.

In addition, specific constraints may be defined, but only at terminal conditions, not during the trajectory path itself. Examples of laws with this kind of constraints include the intercept-angle-control guidance (IACG) [17] and the optimal fixed-interval guidance law (OFIGL) [5].

4.3 Nonlinear robust laws

To tackle the consequences of inaccurate measurements or unmodelled dynamics, in [5] it was proposed to augment the ZEM/ZEV optimal feedback with advancements in the field of nonlinear control. This augmentation is rooted on nonlinear sliding mode control (SMC) theory and the resulting algorithms have been named optimal sliding guidance (OSG) [9, 10]. In this case, a sliding surface is defined as a function of the tracking (zero-effort) errors and a control law is designed to always drive the system asymptotically to that surface. The control law is constructed using Lyapunov's direct method and it can be made very simple and therefore robust.

For the CTVG case, with the sliding surface defined as:

$$\mathbf{s}(t) = \mathbf{ZEV}(t) + \frac{3}{t_{\mathrm{go}}(t)}\mathbf{ZEM}(t) \tag{18}$$

the guidance law becomes:

$$\mathbf{a}(t) = \frac{6}{t_{\mathrm{go}}^2(t)}\mathbf{ZEM}(t) - \frac{2}{t_{\mathrm{go}}(t)}\mathbf{ZEV}(t) - \frac{\phi}{t_{\mathrm{go}}(t)}\operatorname{sign}\mathbf{s}(t) \tag{19}$$

Therefore, we have $k_r = 6$, $k_v = -2$ and:

$$\mathbf{f}\left(\mathbf{ZEM}(t), \mathbf{ZEV}(t), t_{\mathrm{go}}(t)\right) = \frac{1}{t_{\mathrm{go}}(t)}\operatorname{sign}\left\{\mathbf{ZEV}(t) + \frac{3}{t_{\mathrm{go}}(t)}\mathbf{ZEM}(t)\right\} \tag{20}$$

On the other hand, the sliding surface for FTVG laws is simply:

$$\mathbf{s}(t) = \mathbf{ZEM}(t) \tag{21}$$

Therefore, the guidance law becomes:

$$\mathbf{a}(t) = \frac{3}{t_{\mathrm{go}}^2(t)}\mathbf{ZEM}(t) - \frac{\phi}{t_{\mathrm{go}}(t)}\operatorname{sign}\mathbf{s}(t) \tag{22}$$

with $k_r = 3$, $k_v = 0$ and:

$$\mathbf{f}\left(\mathbf{ZEM}(t), \mathbf{ZEV}(t), t_{\text{go}}(t)\right) = \frac{1}{t_{\text{go}}(t)} \text{sign}\, \mathbf{ZEM}(t) \tag{23}$$

In the references mentioned above, it is proven that these guidance algorithms ensure global stability against perturbing accelerations bounded by $||\mathbf{p}(t)||$ by choosing $\phi \geq ||\mathbf{p}(t)||$. This of course comes at the expense of additional control effort.

The main shortcoming of the laws (19) and (22) is that the augmentation with the discontinuous term $\text{sign}\,\mathbf{s}(t)$ can degenerate in the system chattering around the sliding surface, which massively reduces its performance and robustness. To overcome this phenomenon, continuous chattering-free augmentations known as higher-order sliding controllers have been presented over the last years [8, 11]. Details on these recent developments are outside the scope of the paper, which is rather focused on the state-of-practice in Space applications than on SMC theory, and higher-order sliding control terms can also be generically captured by the nonlinear function $\mathbf{f}(.)$.

Finally, as a tabular summary, table 1 presents all the presented planetary descent guidance laws clearly showing their shared commonalities and abstraction into a paremeterised closed-loop guidance general law.

Table 1 Guidance laws for planetary descent

Proportional		
PNG	$\mathbf{a}(t) = nV_c(t)\dot{\Lambda}(t)$	Eq. (13)
APNG	$\mathbf{a}(t) = \frac{n}{t_{\text{go}}^2(t)}\mathbf{ZEM}(t)$	Eq. (14)
Optimal		
CTVG	$\mathbf{a}(t) = \frac{6}{t_{\text{go}}^2(t)}\mathbf{ZEM}(t) - \frac{2}{t_{\text{go}}(t)}\mathbf{ZEV}(t)$	Eq. (16)
FTVG	$\mathbf{a}(t) = \frac{3}{t_{\text{go}}^2(t)}\mathbf{ZEM}(t)$	Eq. (17)
Nonlinear robust		
Sliding CTVG	$\mathbf{a}(t) = \frac{6}{t_{\text{go}}^2(t)}\mathbf{ZEM}(t) - \frac{2}{t_{\text{go}}(t)}\mathbf{ZEV}(t) - \frac{\phi}{t_{\text{go}}(t)}\text{sign}\,\mathbf{s}(t)$	Eq. (19)
Sliding FTVG	$\mathbf{a}(t) = \frac{3}{t_{\text{go}}^2(t)}\mathbf{ZEM}(t) - \frac{\phi}{t_{\text{go}}(t)}\text{sign}\,\mathbf{s}(t)$	Eq. (22)
Parameterised closed-loop guidance		
LOS Kinematics	$\mathbf{a}(t) = \begin{bmatrix} k_r & k_v \end{bmatrix} V_c(t) \begin{bmatrix} \frac{\Lambda(t)}{t_{\text{go}}(t)} \\ \dot{\Lambda}(t) \end{bmatrix} - \phi\,\mathbf{f}\left(\Lambda(t), \dot{\Lambda}(t), t_{\text{go}}(t)\right)$	Eq. (10)
Zero-effort errors	$\mathbf{a}(t) = \begin{bmatrix} k_r & k_v \end{bmatrix} \begin{bmatrix} \frac{\mathbf{ZEM}(t)}{t_{\text{go}}^2(t)} \\ \frac{\mathbf{ZEV}(t)}{t_{\text{go}}(t)} \end{bmatrix} - \phi\,\mathbf{f}\left(\mathbf{ZEM}(t), \mathbf{ZEV}(t), t_{\text{go}}(t)\right)$	Eq. (11)
Open-loop guidance		
Polynomial	$\mathbf{a}(t) = \mathbf{C}_0 + \mathbf{C}_1 t + \ldots + \mathbf{C}_N t^N, \quad N \geq 2$	Eq. (12)

5 Guidance Tuning Example

The purpose of this section is to show how the proposed parametric generalisations of (10) or (11) can be applied for guidance tuning. This preliminary example is particularly focused on providing a general understanding of parametric guidance tuning, thus more advanced tools such as structured $\mathscr{H}_\infty$ optimisation [2, 12] are not yet applied.

This example considers the descent and landing of a spacecraft in Phobos. Its motion (Fig. 1) is simulated by a high-fidelity dynamics model of the Mars-Phobos system, in which the gravity field of the planets is described by a main Keplerian term plus gravity harmonics to account for their inhomogeneity. In addition, uncertainties and variations are included in the gravity field of Phobos by dispersing its gravity harmonics coefficients according to independent normal distributions around their nominal value.

As spacecraft guidance, a CTVG law with zero terminal relative velocity value ($V_c \to 0$ m/s) and state-of-practice gains (16) is implemented. For the estimation of ZEM and ZEV, the apparent acceleration of the spacecraft is instantaneously assumed constant and, to cope with this approximation, the computation of ZEM, ZEV and t_{go} is made with respect to a set of fixed trajectory waypoints designed based on mission analysis considerations.

The result of 1000 Monte-Carlo simulations, starting from a libration point orbit (LPO) over Phobos until touchdown is depicted in Fig. 2. It shows that the same relative velocity response $V_c(t)$ is achieved for all the cases, although the total ΔV (and thus propellant consumption) required for the manoeuvre may range from 13 to 19 m/s, depending on the gravitational perturbations encountered.

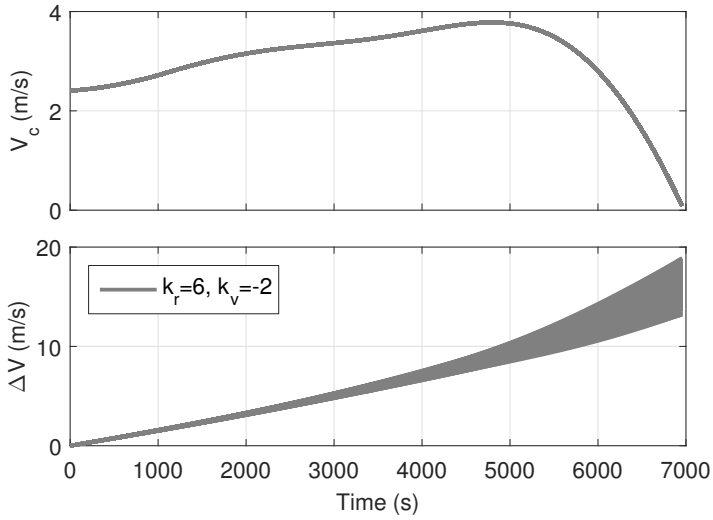

Fig. 2 Phobos descent using CTVG with standard gains (1000 simulations)

As understood from Fig. 2, a successful guidance tuning is translated into an acceptable trade-off between allowable relative velocity and position (not shown) errors versus ΔV. Using results from optimal control theory, the guidance gains of (16) were analytically derived in the literature under the assumption of a simplified and well-known gravitational field.

For the particular scenario addressed in this section, the impact of the guidance gains k_r and k_v is directly analysed by evaluating the nominal value of $V_c(t_f)$ and $\Delta V(t_f)$ over the parameter space. The outcome of this analysis is illustrated in Fig. 3.

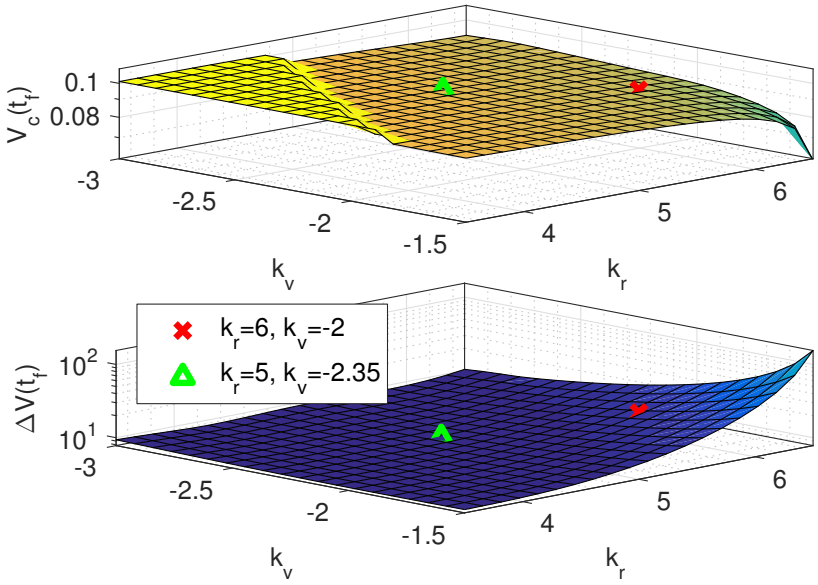

Fig. 3 Tuning trade-offs for Phobos descent using CTVG

Figure 3 provides a clear visualisation of the trade-off between velocity error and ΔV mentioned before: a choice of gains that minimises the error will maximise the ΔV required and vice-versa. However, it also shows that the state-of-practice tuning selection of $k_r = 6, k_v = -2$ (marked with a cross) is not optimal for this scenario. For example, by choosing $k_r = 5, k_v = -2.35$ (marked with a triangle) seems to allow a significant reduction of ΔV while only increasing the velocity error by 0.003 m/s.

In order to validate the observation above, an additional campaign of 1000 Monte-Carlo simulations is performed using the revised guidance gains and keeping the same gravitational perturbations and trajectory waypoints. The comparison of results between standard gains and revised gains (darker lines) is provided in Fig. 4.

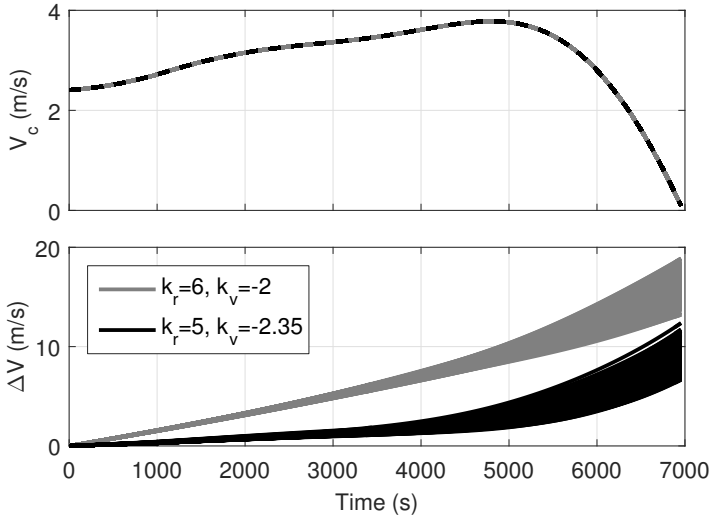

Fig. 4 Phobos descent using CTVG with revised vs. standard gains (1000 simulations)

As anticipated by Fig. 3, the results of Fig. 4 verify that, using the revised gains, the range of ΔV required is significantly reduced, to the interval between 6.5 and 12.5 m/s, while keeping roughly the same dispersion and velocity profile. Moreover, this conclusion confirms that the traditional analytical choice of gains may no longer be optimal in the case of complex and perturbed gravitational environments. This type of behaviour is one of the main motivations of the project under which this study was developed to exploit the application of systematic non-smooth optimisation tools such as [2, 12].

6 Conclusions

After providing an overview of state-of-the-art techniques for planetary descent, the main conclusion of this paper is that different groups of guidance laws can be generalised as functions of a set of tunable parameters. This parameterisation is highlighted in (10) and (11) and it is very convenient for the design of fixed-structure GNC architectures for planetary landers. An example of guidance tuning focusing on this fixed-structure is also provided in Sec. 5. Work on the project under which this study was developed is now continuing with the generation of models that capture the highly uncertain environment of small planetary bodies and with the tuning of the parameterised laws to be robust against those uncertainties using novel non-smooth $\mathscr{H}_\infty$ optimisation methods.

References

1. B. Açikmeşe and S. Ploen. A Powered Descent Guidance Algorithm for Mars Pinpoint Landing. In *The 2005 AIAA Guidance, Navigation, and Control Conference*, San Franciso, CA, Aug 15–18 2005.
2. P. Apkarian, M. Dao, and D. Noll. Parametric robust structured control design. *Transactions on Automatic Control*, 60(7):1857–1869, 2015.
3. R. Battin. *An Introduction to the Mathematics and Methods of Astrodynamics*. AIAA Education Series, 1st edition, 1987.
4. C. D'Souza. An optimal guidance law for planetary landing. In *The 1997 AIAA Guidance, Navigation, and Control Conference*, New Orleans, LA, Aug 11–13 1997.
5. B. Ebrahimi, M. Bahrami, and J. Roshanian. Optimal sliding-mode guidance with terminal velocity constraint for fixed-interval propulsive maneuvers. *Acta Astronautica*, 62(10):556–562, 2008.
6. A. Falcoz, C. Pittet, S. Bennani, A. Guignard, C. Bayart, and B. Frapard. Systematic design methods of robust and structured controllers for satellites. *Space Journal*, 7(3):319–334, 2015.
7. F. Ferrari, M. Lavagna, M. Scheper, B. Burmann, and I. Carnelli. The European Asteroid Impact Mission: Phase A Design and Mission Analysis. In *The 2015 AAS/AIAA Astrodynamics Specialist Conference*, Vail, CO, Aug 9–13 2015.
8. R. Furfaro, D. Cersosimo, and D. Wibben. Asteroid Precision Landing via Multiple Sliding Surfaces Guidance Techniques. *Journal of Guidance, Control, and Dynamics*, 36(4):1075–1092, 2013.
9. R. Furfaro, B. Gaudet, D. Wibben, and J. Simo. Development of Non-Linear Guidance Algorithms for Asteroids Close-Proximity Operations. In *The 2013 AIAA Guidance, Navigation, and Control Conference*, Boston, MA, Aug 19–22 2013.
10. R. Furfaro, S. Selnick, M. Cupples, and M. Cribb. Non-Linear Sliding Guidance Algorithms for Precision Lunar Landing. In *The 2011 AAS/AIAA Spaceflight Mechanics Meeting*, New Orleans, LA, Feb 13–17 2011.
11. R. Furfaro, D. Wibben, B. Gaudet, and J. Simo. Terminal Multiple Surface Sliding Guidance for Planetary Landing: Development, Tuning and Optimization via Reinforcement Learning. *Journal of the Astronautical Sciences*, 62(1):73–99, 2015.
12. P. Gahinet and P. Apkarian. Structured H_∞ Synthesis in MATLAB. In *The 18th IFAC World Congress*, Milan, Italy, Aug 28–Sep 02 2011.
13. K. Geurts, C. Fantinati, S. Ulamec, and R. Willnecker. Rosetta Lander: On-Comet Operations Preparation and Planning. In *The AIAA SpaceOps 2014 Conference*, Passadena, CA, May 5–9 2014.
14. J. Gil-Fernandez, R. Panzeca, and C. Corral. Impacting small Near Earth Objects. *Advances in Space Research*, 42(8):1352–1363, 2008.
15. Y. Guo, M. Hawkins, and B. Wie. Optimal Feedback Guidance Algorithms for Planetary Landing and Asteroid Intercept. In *The 2011 AAS/AIAA Astrodynamics Specialist Conference*, Girdwood, AK, Jul 31–Aug 4 2011.
16. Y. Guo, M. Hawkins, and B. Wie. Applications of Generalized Zero-Effort-Miss/Zero-Effort-Velocity Feedback Guidance Algorithm. *Journal of Guidance, Control, and Dynamics*, 36(3):810–820, 2013.
17. M. Hawkins, Y. Guo, and B. Wie. Guidance algorithms for asteroid intercept missions with precision targeting requirements. In *The 2011 AAS/AIAA Astrodynamics Specialist Conference*, Girdwood, AK, Jul 31–Aug 4 2011.
18. M. Hawkins, Y. Guo, and B. Wie. Spacecraft Guidance Algorithms for Asteroid Intercept and Rendezvous Missions. *International Journal of Aeronautical and Space Sciences*, 13(2):154–169, 2012.
19. M. Hawkins, A. Pitz, and B. Wie. Terminal-Phase Guidance and Control Analysis of Asteroid Interceptors. In *The 2010 AIAA Guidance, Navigation, and Control Conference*, Toronto, Canada, Aug 2–5 2010.
20. A. Klumpp. Apollo lunar descent guidance. *Automatica*, 10(2):133–146, 1974.

21. D. Kubitschek. Impactor spacecraft targeting for the Deep Impact mission to comet Temple 1. In *The 2003 AAS/AIAA Astrodynamics Specialist Conference*, Big Sky, MT, Aug 3–7 2003.
22. M. Lara and D. Scheeres. Stability bounds for three-dimensional motion close to asteroids. *Journal of the Astronautical Sciences*, 50(4):389–409, 2003.
23. D. Lauretta and OSIRIS-REx Team. An Overview of the OSIRIS-REx Asteroid Sample Return Mission. In *The 43rd Lunar and Planetary Science Conference*, Woodlands, TX, Mar 19–23 2012.
24. S. Li and X. Jiang. Review and prospect of guidance and control for Mars atmospheric entry. *Progress in Aerospace Sciences*, 69:40–57, 2014.
25. P. Lunghi, M. Lavagna, and R. Armellin. Semi-Analytical Adaptive Guidance Algorithm for Fast Retargeting Maneuvers Computation During Planetary Descent and Landing. In *The 12th Symposium on Advanced Space Technologies in Robotics and Automation*, Noordwijk, Netherlands, May 15–17 2013.
26. A. Marcos and S. Bennani. LPV Modeling, Analysis and Design in Space Systems: Rationale, Objectives and Limitations. In *The 2009 AIAA Guidance, Navigation, and Control Conference*, Chicago, IL, Aug 10–13 2009.
27. D. Vallado. *Fundamentals of Astrodynamics and Applications*. Microcosm Press, 3rd edition, 2007.
28. E. Wong, G. Singh, and J. Masciarelli. Guidance and Control Design for Hazard Avoidance and Safe Landing on Mars. *Journal of Spacecraft and Rockets*, 43(2):378–384, 2006.
29. T. Yoshimitsu, J. Kawaguchi, T. Hashimoto, T. Kubota, M. Uo, H. Morita, and K. Shirakawa. Hayabusa – final autonomous descent and landing based on target marker tracking. *Acta Astronautica*, 65(5):657–665, 2009.
30. P. Zarchan. *Tactical and Strategic Missile Guidance*. AIAA Progress in Astronautics and Aeronautics, 2nd edition, 1994.
31. K. Zhou, J. Doyle, and K. Glover. *Robust and Optimal Control*. Prentice-Hall, 1st edition, 1995.